REFERENCES

[1] E. L. Briggs, D. J. Sullivan and J. Bernholc, Phys. Rev. B **52**, R5471 (1995); Phys. Rev. B **54**, 14362 (1996).

[2] J. Perdew and A. Zunger, Phys. Rev. B **23**, 5048 (1981).

[3] L. Kleinman and D. Bylander, Phys. Rev. Lett. **48**, 1425 (1982).

[4] G. Bachelet, D. Hamann and M. Schlüter, Phys. Rev. B **26**, 4199 (1982).

[5] D. Hamann, M. Schlüter and C. Chiang, Phys. Rev. Lett. **43**, 1494 (1979).

[6] D. Hamann, Phys. Rev. B **40**, 2980 (1989).

[7] M. Buongiorno Nardelli, K. Rapcewicz and J. Bernholc, Phys. Rev. B **55**, R7323 (1997).

[8] A. Baldereschi, S. Baroni and R. Resta, Phys. Rev. Lett. **61**, 734 (1988).

[9] M. Posternak, A. Baldereschi, A. Catellani and R. Resta, Phys. Rev. Lett. **64**, 1777 (1990).

[10] K. Shiraishi, J. Phys. Soc. Jap. **59**, 3455 (1990).

[11] H. Morkoç, S. Strite, G.B. Gao, M.E. Lin, B. Sverdlov, and M. Burns, J. Appl. Phys. **76**, 1363 (1994).

[12] L. Calcagnile, G. Coli, M. De Vittorio, R. Rinaldi, P. V. Di Giugno, R. Cingolani, L. Vanzetti, L. Sorba and A. Franciosi, J. of Crystal Growth, **159**, 793 (1996).

[13] A. Miller, D. Chemla, T. Damen, A. Gossard, W. Weigman, T. Wood and C. Burrus, Phys. Rev. B **32**, 1043 (1985).

[14] G. Bastard, E. Mendez, L.Chang and L. Esaki, Phys. Rev. B **28**, 3241 (1983).

[15] M. Buongiorno Nardelli, K. Rapcewicz and J. Bernholc, Appl. Phys. Lett. **27**, in press (1997).

[16] Y. Narukawa, Y. Kawakami, S. Fujita, S. Fujita, and S. Nakamura, Phys. Rev. B **55**, R1938 (1997).

[17] K. Rapcewicz, M. Buongiorno Nardelli and J. Bernholc, Phys. Rev. B **56**, R12725 (1997).

[18] M. M. Sung, J. Ahn, V. Bykov, J. W. Rabalais, D. D. Koleske and A. E. Wickenden, Phys. Rev. B **54**, 14652 (1996).

[19] S. S. Dhesi, C. B. Stagarescu, K. E. Smith, R. Singh and T. D. Moustakas, Phys. Rev. B **56**, 10271 (1997).

[20] S. Guha, N. A. Bojarczuk and F. Cardone, Appl. Phys. Lett. **71**, 1685 (1997).

THEORETICAL STUDY OF NATIVE POINT DEFECTS IN AlN AND InN

C. STAMPFL and CHRIS G. VAN DE WALLE

Xerox PARC, 3333 Coyote Hill Road, Palo Alto, CA 94304

ABSTRACT

We have studied native point defects in AlN and InN using density-functional calculations employing both the local-density and generalized gradient approximations for the exchange-correlation functional. For both materials we find that the nitrogen vacancy acts as a compensating center in p-type material. For AlN in the zinc-blende structure, the aluminum interstitial has an equally low formation energy as the nitrogen vacancy. For n-type material the aluminum vacancy is the dominant compensating center in AlN. For n-type InN, all defect formation energies are high.

INTRODUCTION

Much progress has been made in the growth and fabrication of optoelectonic devices based on III-V nitrides [1-3]. The particular material properties responsible for this interest are the large band gaps and very strong interatomic bonds. Further investigations are still required, however, for example concerning the control of doping levels; the issues include suppression of background n-type conductivity, achieving and understanding n- and p-type doping of AlGaN alloys, and compensation effects by native defects. Valuable insight into such problems can be obtained from first-principles calculations which provide information about the atomic and electronic structure, formation energies, and compensation effects.

In the present work we have studied all native point defects in the relevant charge states in AlN and InN. The character and behavior of the defects are in many ways similar to those which have been reported in GaN [4,5]. We find, however, several important differences which have implications for compensation issues. We also compare results obtained using the local-density approximation (LDA) [6] and the generalized gradient approximation (GGA) [7] for the exchange-correlation functional.

Below we give a brief description of the theoretical method and discuss our results for AlN and InN in the two subsequent sections. We then compare LDA and GGA results. The final section contains the conclusions.

THEORETICAL METHOD

The calculations are performed using the density-functional pseudopotential method [8]. The wave functions are expanded in a plane-wave basis set and the system modeled using the supercell approach. We employ a tight-binding initialization scheme for the electronic wave functions to improve convergence. The soft pseudopotentials are created using the scheme of Troullier and Martins [9], and for the GGA calculations we include the GGA in creation of the pseudopotential as well as in the self-consistent total energy calculations so that the description is consistent [10]. We primarily treat the indium $4d$ electrons using the non-linear core correction (nlcc) introduced by Louie *et al.* [11]. For several defects we have also performed calculations including the $4d$ electrons as valence states, confirming our results. The majority of the calculations are performed using 32-atom zinc-blende

Mat. Res. Soc. Symp. Proc. Vol. 482 © 1998 Materials Research Society

supercells. We have also investigated low-energy defects in the wurtzite structure, using 72-atom supercells. We relax the positions of the atoms around the defect using a damped dynamics approach [8].

The formation energy of a defect in charge state q is obtained as

$$E^f(q) = E^{\rm tot}_{\rm defect}(q) - \sum_{\rm X} n_{\rm X}\mu_{\rm X} + qE_{\rm F} \quad , \tag{1}$$

where $E^{\rm tot}_{\rm defect}(q)$ is the total energy of the defect system, and $n_{\rm X}$ and $\mu_{\rm X}$ are the number and chemical potential of atoms of species X, respectively. $E_{\rm F}$ is the Fermi energy which is set to zero at the valence-band maximum. We assume thermal equilibrium, requiring $\mu_{\rm Al} + \mu_{\rm N} = \mu_{\rm AlN}$ or $\mu_{\rm In} + \mu_{\rm N} = \mu_{\rm InN}$. The chemical potentials depend on the experimental growth conditions. In the following we consider either metal- or N-rich conditions. In metal-rich conditions we set $\mu_{\rm Al}$ (or $\mu_{\rm In}$) equal to the energy of bulk Al (or bulk In); in N-rich conditions the chemical potential is determined by the energy of an N_2 molecule.

NATIVE DEFECTS IN AlN

Figure 1 summarizes all the defect formation energies as calculated under N- and Al-rich conditons in zinc-blende AlN. We consider $E_{\rm F}$ spanning the zinc-blende band gap of 5.0 eV (as obtained from quasiparticle calculations [12]). Our calculated LDA indirect gap $(\Gamma_{15} - X_1)$ for zinc-blende AlN is 3.2 eV; the gap at Γ is 4.3 eV. The change in slope of the lines in Fig. 1 represents a change in the charge state of the defect [cf. Eq. 1]. The lowest energy defects are the nitrogen ($V_{\rm N}$) and aluminum ($V_{\rm Al}$) vacancies, as well as the aluminum interstitial ($\rm Al_i$). Under n-type conditions $V_{\rm Al}$ (a triple acceptor) dominates; under p-type conditions, $V_{\rm N}$ and $\rm Al_i$ (both triple donors) dominate. For the wurtzite structure our calculations show that the N- and Al-vacancies behave qualitatively very similarly to the zinc-blende material. The aluminum interstitial, however, behaves differently in the two materials due to the different local atomic geometry of the site. In particular, we find that the formation energy in wurtzite material is more than 2 eV higher than in zinc-blende material. For the nitrogen vacancy only the $V_{\rm N}^{+}$ and $V_{\rm N}^{3+}$ charge states are stable; the $V_{\rm N}^{2+}$ state is unstable, thus presenting a negative-U effect. Furthermore, it can be seen that the formation energy of the nitrogen vacancy in n-type material is sufficiently high for this defect not to occur in high concentrations.

The defect formation energies in p-type AlN are notably lower than those of the corresponding point defects in GaN, particularly under Al-rich conditions; this can be attributed to the wider band gap of AlN as compared to GaN. This suggests that compensation effects are likely to be more pronounced in AlN. In particular, compensation of acceptors by the nitrogen vacancy becomes increasingly important in $\rm Al_xGa_{1-x}N$ alloys with increasing x. Difficulties in achieving p-type doping of $\rm Al_xGa_{1-x}N$ for $x > 0.1$ have indeed been reported in the literature [13].

In n-type AlN the formation energy of the cation vacancy ($V_{\rm Al}$) is also lower than for the corresponding defect in GaN ($V_{\rm Ga}$). Once again, the degree of compensation and corresponding reduction in n-type conductivity will increase with alloy composition x. n-type $\rm Al_xGa_{1-x}N$ has been reported to exhibit a dramatic decrease in the free carrier concentration for $x > 0.4$ [15,16]. We propose that two effects are responsible for this behavior: (i) in the case of doping with oxygen (the most common unintentional donor), a DX transition occurs which converts the shallow donor into a deep level [16]; and (ii) compensation by the cation vacancy ($V_{\rm Ga}$ or $V_{\rm Al}$), a triple acceptor, increases with alloy composition x.

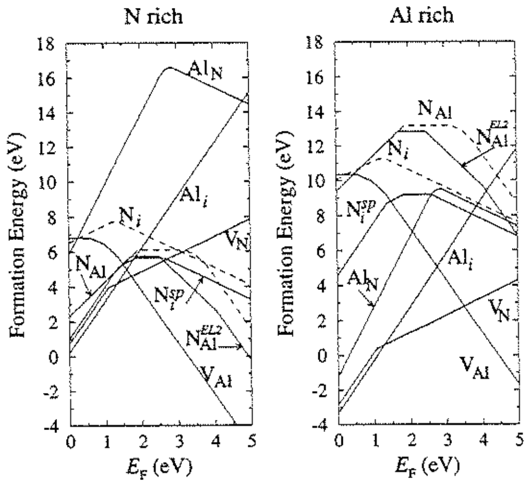

Figure 1: Formation energies of native defects in zinc-blende AlN as a function of the Fermi level under nitrogen-rich (left panel) and aluminum-rich (right panel) conditions. $E_{\rm F} = 0$ corresponds to the valence-band maximum.

Figure 1 shows that formation energies of native point defects other than the vacancies and the Al interstitial are very high, hence those defects are unlikely to occur in significant concentrations. As for GaN [4] we find that the nitrogen split interstitial ($\rm N_i^{sp}$) has a lower formation energy than the high-symmetry tetrahedral interstitial site ($\rm N_i$) with four Al neighbors. Also note that the nitrogen antisite ($\rm N_{Al}^{EL2}$) prefers an $EL2$-like geometry for the negative charge states, in agreement with the findings of Ref. [17].

NATIVE DEFECTS IN InN

InN is probably the least studied of the III-V nitrides, in part because of the difficulty in preparing the material due to its low thermal stability. InN, however, represents an important constituent in group III-nitride materials and devices, since $\rm In_xGa_{1-x}N$ is often used as the active layer in short-wavelength light emitters. Increasing the In content in InGaN makes it possible, in principle, to extend the light emitting range from violet to red.

To our knowledge this is the first *ab initio* study of defects in InN. For InN the underestimation of the band gap as obtained within the LDA is more severe than in GaN and AlN (the LDA gap at Γ is negative); due to this difficulty, our calculated formation energies may not be as reliable as those for AlN. Nevertheless, we are confident that the qualitative conclusions mentioned below are correct. In the left and right panels of Fig. 2 the defect formation energies for N- and In-rich conditions are shown as a function of the Fermi level. Here $E_{\rm F}$ spans the experimental band gap of wurtzite InN (1.9 eV). We use the wurtzite value since there has been no accurate experimental determination of the zinc-blende band gap that we are aware of. We note that the differences between N-rich and In-rich material are small, due to the small heat of formation of InN.

Figure 2 shows that the nitrogen vacancy is the defect with the lowest formation energy; it will act as a compensating center in p-type InN (and InGaN alloys). As for AlN described above, the N vacancy in InN exhibits a negative-U effect between the $V_{\rm N}^{3+}$ and $V_{\rm N}^{+}$ charge states. Under n-type conditions (large $E_{\rm F}$) all native defects have high formation energies. We conclude that the dominant native point defect in InN is the nitrogen vacancy.

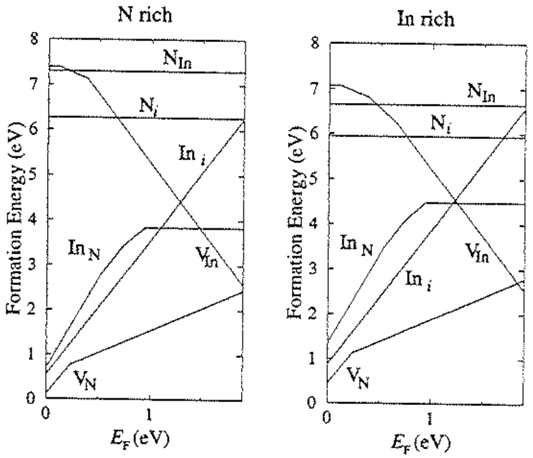

Figure 2: Formation energies of native defects in zinc-blende InN as a function of the Fermi level under nitrogen-rich (left panel) and aluminum-rich (right panel) conditions. $E_F = 0$ corresponds to the valence-band maximum. For N_{In} and N_i only the neutral charge state was investigated.

METHODOLOGICAL ASPECTS

The generalized gradient approximation (GGA) is an improved version of the exchange-and-correlation functional that enters in density-functional theory. It has been shown to yield improvements over the local-density approximation (LDA), most notably for total energies and atomization energies of molecules [7], adsorption energies [18], activation barriers for H_2 dissociation [19], and reaction energies [20]. The GGA has also been reported to improve the band structure of transition metal oxides [21]. We therefore considered it worthwhile to compare LDA and GGA results for the III-V nitrides, for bulk properties as well as formation energies of native defects. To our knowledge no previous GGA calculations for defect formation energies in semiconductors have been performed.

In Table 1 we show calculated and experimental values for bulk Al and the N_2 dimer. The energy cutoffs were 40 Ry for bulk Al and 70 Ry for N_2. For both systems the GGA leads to a significant improvement over the LDA results, in particular for the cohesive and binding energies. These energies are important quantities since bulk Al and the N_2 dimer serve as our reservoirs in the calculation of defect formation energies in AlN. Table 2 shows our LDA and GGA results for lattice constants, bulk moduli, and cohesive energies of AlN, GaN, and InN. These calculations were performed using an energy cutoff of 80 Ry and with the *d*-electrons of the Ga and In atoms included as valence electrons. For AlN the GGA yields some improvement in the lattice constant; the cohesive energy is also in markedly better agreement with experiment. The LDA, on the other hand, overbinds by $\approx$1.6 eV. For GaN and InN, however, the GGA does not produce any improvement: The GGA lattice constants are larger than the LDA values (which are larger than experiment already). With respect to the cohesive energies, the LDA *overbinds* GaN and InN by about 1 eV while the GGA tends to *underbind* by a similar amount.

	Al bulk			N_2 dimer		
	a(Å)	B(Mbar)	E_c(eV)	d(Å)	ν(cm^{-1})	E_b(eV)
LDA	3.96	0.83	4.03	1.10	2384	11.59
GGA	4.04	0.74	3.42	1.11	2346	9.87
Expt. [22]	4.05	0.773	3.39	1.10	2360	9.9

Table 1: Calculated lattice constant, a, bulk modulus, B, and cohesive energy, E_c, of bulk Al. Bond length, d, frequency, ν, and binding energy, E_b, for the N_2 dimer.

	AlN			GaN			InN		
	a(Å)	B (Mbar)	E_c (eV)	a	B	E_c	a	B	E_c
LDA	4.31	2.06	13.24	4.52	1.91	10.18	5.00	1.40	8.68
GGA	4.39	1.91	11.36	4.59	1.56	8.25	5.11	1.17	6.86
Expt. [22]	4.38	2.02	11.67	4.49	1.90	9.06	4.97	1.37	7.97

Table 2: Calculated lattice constants, a, bulk moduli, B, and cohesive energies, E_c, of zinc-blende AlN, GaN, and InN. Experimental values for cohesive energies are for wurtzite material; values for the zinc-blende structure are expected to be smaller by a few 0.01 eV.

We also carefully studied whether the use of the GGA would produce any change in the band structure. The LDA and GGA band structures are actually extremely similar, at least when they are calculated at the same lattice constant. At the *experimental* lattice constant the LDA and GGA band gaps differ by less than 0.02 eV. The band structures at the respective *theoretical* lattice constants (see Table 2) do exhibit differences, essentially due to deformation-potential effects. Our calculated GGA-band-gaps at the *theoretical* lattice constants are 0.62 eV (for AlN) and 0.31 eV (for GaN) smaller than the LDA band gaps. Since our point-defect calculations are always carried out at the *theoretical* lattice constant (to avoid spurious relaxations) these differences in band structure may affect energies for defects which have occupied levels in the band gap.

We have performed calculations for selected neutral and charged native point defects in AlN and InN using the GGA. We found that the formation energies are in general qualitative agreement with the LDA; in particular, all of the conclusions regarding dominance of point defects and their tendency to compensate are unaffected by the use of the GGA. However, some quantitative differences do exist. We were able to attribute these differences to two main effects: (i) defect-induced levels lie at a lower energy in the GGA due to the smaller band gap, as discussed above; and (ii) the energies of the reservoirs [chemical potentials; see Eq. (1)] differ due to the LDA/GGA differences in the cohesive energies (and heats of formation). Further details of these results will be reported in a forthcoming publication.

CONCLUSIONS

We have performed first-principles calculations for native point defects in AlN and InN. In both materials the nitrogen vacancy has the lowest formation energy in *p*-type material. In addition, in *cubic* AlN the aluminum interstitial has an equally low formation energy as the N vacancy. These defects may therefore act to compensate acceptors. In *n*-type AlN, the aluminum vacancy has the lowest formation energy and is likely to serve as an effective compensating center for donors. Furthermore, in n-type AlN and InN the nitrogen vacancy has a high formation energy indicating low concentrations. The formation energies of native defects are found to be qualitatively similar in LDA and GGA.

ACKNOWLEDGEMENTS

This work was supported in part by DARPA under agreement no. MDA972-96-3-014. C. Stampfl acknowledges support from the DFG (Deutsche Forschungsgemeinschaft).

REFERENCES

1. H. Morkoç, S. Strite, G. B. Gao, M. E. Lin, B. Sverdlov, and M. Burns, J. Appl. Phys. **76**, 1363 (1994).
2. F. A. Ponce and D. P. Bour, Nature **386**, 351 (1997), and references therein.
3. S. Nakamura, Solid State Commun. **102**, 237 (1997), and references therein.
4. J. Neugebauer and C. G. Van de Walle, Phys. Rev. B **50**, 8067 (1994).
5. P. Boguslawski, E. L. Briggs, and J. Bernholc, Phys. Rev. B **51**, 17255 (1995).
6. D. M. Ceperley and B. I. Alder, Phys. Rev. Lett. **45**, 556 (1980); P. Perdew and A. Zunger, Phys. Rev. B **23**, 5048 (1981).
7. J. P. Perdew, J. A. Chevay, S. H. Vosko, K. A. Jackson, M. R. Pederson, D. J. Singh, and C. Fiolhais, Phys. Rev. B **46**, 6671 (1992).
8. M. Bockstedte, A. Kley, J. Neugebauer, and M. Scheffler, Comp. Phys. Commun., to be published.
9. N. Troullier and J. L. Martins, Phys. Rev. B **43**, 1993 (1991).
10. M. Fuchs and M. Scheffler, to be published.
11. S. G. Louie, S. Froyen, and M. L. Cohen, Phys. Rev. B **26**, 1738 (1982).
12. A. Rubio, J. L. Corkhill, M. L. Cohen, E. Shirley, and S. G. Louie, Phys. Rev. B **48**, 11810 (1993).
13. M. D. Bremser, W. G. Perry, T. Zheleva, N. V. Edwards, O. H. Nam, N. Parikh, D. E. Aspnes, and R. F. Davis, MRS Internet J. Nitride Semicond. Res. **1**, 8 (1996).
14. H. G. Lee, M. Gershenzon, and B. L. Goldenberg, J. Elec. Mat. **20**, 621 (1991).
15. X. Zhang, P. Kung, A. Saxler, D. Walker, T. C. Wang, and M. Razeghi, Appl. Phys. Lett. **67**, 1745 (1995).
16. C. G. Van de Walle, Phys. Rev. B (in press).
17. T. Mattila, A. P. Seitsonen, and R. M. Nieminen, Phys. Rev. B **54**, 1474 (1996).
18. P. H. T. Philipsen, G. te Velde, and E. J. Baerands, Chem. Phys. Lett. **226**, 583 (1994).
19. B. Hammer, K. W. Jacobsen, and J. K. Norskov, Phys. Rev. Lett. **70**, 3971 (1993).
20. D. Porezag and M. R. Pederson, J. Chem. Phys. **102**, 9345 (1995).
21. P. Dufek, P. Blaha, V. Sliwko, and K. Schwarz, Phys. Rev. B **49**, 10170 (1994).
22. Bulk Al from C. Kittel, *Introduction to Solid State Physics*, 6th ed. (Wiley, New York, 1986); N_2 from A. D. Becke in *Density Functional Theories in Quantum Chemistry*; Cohesive energies of AlN, GaN, and InN from B. Paulus *et al.*, J. Phys: Condens. Mat. **9**, 2745 (1997). Lattice constants from *Properties of Group III-Nitrides*, edited by J. H. Edgar, EMIS Datareviews Series (London, 1994). Bulk moduli from M. E. Sherwin *et al.*, J. Appl. Phys. **69**, 8423 (1991), calculated from a transformation of the wurtzite elastic constants.

BAND OFFSETS IN GaN/AlN AND AlN/SiC HETEROJUNCTIONS

NADIA BINGGELI*, PHILIPPE FERRARA**, ALFONSO BALDERESCHI*

*Institut de Physique Appliquée, Ecole Polytechnique Fédérale de Lausanne, CH-1015 Lausanne, Switzerland
**Biochemisches Institut der Universität Zürich, CH-8057 Zürich, Switzerland

ABSTRACT

We have investigated the structural trends of the band offsets in GaN/AlN and AlN/SiC heterojunctions using the *ab initio* pseudopotential method. In the zincblende GaN/AlN (100), (110), and (111) heterojunctions, the band offsets are relatively insensitive to interface orientation. Bulk strain effects, however, can modify the offset by as much as 0.4 eV in coherently strained AlN/GaN and GaN/AlN (100) junctions. The band alignment in the heterovalent AlN/SiC (110) and (111) heterojunctions depends on the geometry and stoichiometry of the interface. Valence band offsets as high as 2.5 eV are obtained for neutral AlN/SiC(111) junctions with a mixed Al/Si interface layer and as low as 1.3 eV with a mixed N/C layer. Atomic relaxation plays a major role in determining the offset. The change from zincblende (111) to wurtzite (0001) crystal structure in GaN/AlN and AlN/SiC heterojunctions selectively affects the conduction band offset, and has only a minor influence on the valence discontinuity.

INTRODUCTION

The group-III nitrides and SiC are materials of considerable interest for novel device applications in blue-violet optoelectronics and high-temperature electronics. SiC is also one of the substrates of choice for the growth of GaN– and AlN–based devices. Although lately there has been considerable progress in understanding and controlling the bulk properties of these wide-gap materials, the situation is less satisfactory as far as their interface properties are concerned. In particular, few experimental or theoretical data are available on the band offsets that control carrier injection and confinement in nitride heterojunctions, and little is known on their trends as compared to other semiconductor heterojunctions.

Here we examine from first principles the structural trends of the band offsets in nitride heterojunctions, including the offset dependence on interface orientation, strain, and polytype. As prototype systems we selected the isovalent GaN/AlN and the heterovalent AlN/SiC heterojunctions in the zincblende (3C) and wurtzite (2H) crystalline forms.

METHOD

The *ab initio* calculations were performed within the local-density approximation to density-functional theory, using Troullier-Martins pseudopotentials and a plane-wave basis set [1]. The Ga-3d orbitals were treated as valence states. We also carried out, however, some calculations with the Ga-3d states in the core in order to assess their influence on the band offsets. To evaluate the valence–band offset (VBO), we used the technique described in Ref. [2]. The interfaces were modeled with supercells containing 12 atomic layers for the (110) junctions and 24 atomic layers for the (100), (111) and (0001) junctions. The supercell

Mat. Res. Soc. Symp. Proc. Vol. 482 © 1998 Materials Research Society